International Journal of Mass Spectrometry 290 (2010) 106–112

Contents lists available at ScienceDirect

International Journal of Mass Spectrometry

journal homepage: www.elsevier.com/locate/ijms

FA-SIFT study of reactions of protonated water and ethanol clusters with α-pinene and linalool in view of their selective detection by CIMS

F. Dhooghe[a,b], C. Amelynck[a,*], J. Rimetz-Planchon[a], N. Schoon[a], F. Vanhaecke[b]

[a] Belgian Institute for Space Aeronomy, Ringlaan 3, B-1180 Brussels, Belgium
[b] Department of Analytical Chemistry, Ghent University, Krijgslaan 281, S12, B-9000 Ghent, Belgium

ARTICLE INFO

Article history:
Received 3 November 2009
Received in revised form 3 December 2009
Accepted 15 December 2009
Available online 23 December 2009

Keywords:
FA-SIFT
CIMS
Ion/molecule reactions
Linalool
Monoterpene

ABSTRACT

The use of protonated water clusters and protonated ethanol clusters as reagent ions has been evaluated for the resolution of an interference encountered in CIMS when measuring monoterpenes ($C_{10}H_{16}$) and linalool ($C_{10}H_{18}O$) simultaneously.

To this end, the reactions of $H_3O^+\cdot(H_2O)_n$ (n = 1–3), $(C_2H_5OH)_mH^+$ (m = 1–3) and $(C_2H_5OH\cdot H_2O)H^+$ with α-pinene and linalool have been characterized in a flowing afterglow-selected ion flow tube (FA-SIFT) instrument at a SIFT He buffer gas pressure of 1.43 hPa and a temperature of 298 K.

All reactions with linalool were found to occur at the collision limit. The reaction of $(C_2H_5OH)_2H^+$ with α-pinene proceeds at half the collision rate and both the reactions of $(C_2H_5OH)_3H^+$ and $H_3O^+\cdot(H_2O)_3$ with α-pinene have a very low rate constant. All other reactions involving α-pinene proceed at the collision rate.

The reactions of $H_3O^+\cdot H_2O$, $H_3O^+\cdot(H_2O)_2$, $C_2H_5OH_2^+$, $(C_2H_5OH\cdot H_2O)H^+$ and $(C_2H_5OH)_2H^+$ with α-pinene mainly proceed by proton transfer. Additionally, ligand switching channels have been observed for the reactions of $(C_2H_5OH)_2H^+$ and $H_3O^+\cdot(H_2O)_2$ with α-pinene.

Protonated linalool was observed as a minor product for the reactions of $(C_2H_5OH\cdot H_2O)H^+$ and $H_3O^+\cdot(H_2O)_n$ (n = 1–3) with linalool. For all linalool reactions, a contribution of the dissociative proton transfer product at m/z 137 was found and this ion was the main product ion for the reactions with $H_3O^+\cdot H_2O$, $C_2H_5OH_2^+$ and $(C_2H_5OH\cdot H_2O)H^+$. For the $(C_2H_5OH\cdot H_2O)H^+$/linalool reaction, ligand switching with both water and ethanol has been observed. Major ligand switching channels were observed for the reactions of $(C_2H_5OH)_2H^+$, $(C_2H_5OH)_3H^+$ and $H_3O^+\cdot(H_2O)_2$ with linalool. Also, for the $H_3O^+\cdot(H_2O)_3$/linalool reaction, several ligand switching channels have been observed.

These results are discussed in view of their applicability for the selective detection of monoterpenes and linalool with CIMS instrumentation such as SIFT-MS, PTR-MS and APCI-MS.

1. Introduction

During the last decade, chemical ionization mass spectrometry (CIMS) has become a widely used, fast and sensitive technique for on-line quantification of non-methane biogenic volatile organic compounds (BVOC). BVOCs emitted by terrestrial vegetation are of interest to environmental scientists because of their large emission rates [1], their fast reaction rates with the main atmospheric oxidants ($OH^\bullet$, O_3 and $NO_3^\bullet$) and the health effects associated with the reaction products formed from these reactions in the presence of NO_x (O_3, secondary organic aerosol (SOA)) [2–4]. Compounds that are emitted from vegetation comprise isoprene (C_5H_8), monoterpenes ($C_{10}H_{16}$), sesquiterpenes ($C_{15}H_{24}$) and oxygenated terpenes as some of the major groups.

CIMS techniques use selective reactions between specific reactant ions – that do not react with the main atmospheric constituents – and the trace gas of interest, resulting in specific product ions that are fingerprints of the compounds to be detected. A very popular reactant ion in CIMS techniques for trace gas detection is the hydronium ion (H_3O^+). It is used in the well-established medium-pressure proton transfer reaction-mass spectrometry (PTR-MS) [5] and selected ion flow tube-mass spectrometry (SIFT-MS) [6] techniques, as well as in atmospheric pressure chemical ionization-mass spectrometry (APCI-MS) [7]. In all three techniques, the H_3O^+ ions rapidly form $H_3O^+\cdot(H_2O)_n$ cluster ions when quantification of BVOCs is carried out in ambient (humid) air samples. At standard drift field conditions in PTR-MS (E/N = 120–130 Td with E = applied drift field, N = buffer gas number density in the reactor, 1 Td = 10^{-17} V cm^2 molecule^{-1}), the

* Corresponding author. Tel.: +32 2 373 03 90; fax: +32 2 373 84 23.
E-mail address: crist.amelynck@aeronomie.be (C. Amelynck).

1387-3806/$ – see front matter © 2009 Elsevier B.V. All rights reserved.
doi:10.1016/j.ijms.2009.12.010

proton hydrate distribution is mainly restricted to bare H_3O^+ ions (>90%).

In the present paper, the focus lies on resolving an isobaric interference occurring when measuring monoterpenes ($C_{10}H_{16}$) and linalool ($C_{10}H_{18}O$) simultaneously with CIMS instrumentation. This problem was encountered in recent PTR-MS measurements, aiming at the quantification of monoterpene emissions from *Fagus Sylvatica* L. trees in growth chamber experiments in the framework of the IMPECVOC project (www.impecvoc.be). This interference could be expected, as the major ions reported for the H_3O^+/monoterpene reactions have an m/z value of 137 (protonated monoterpene) and 81 (fragment ion) [8–11] and the major ones for the H_3O^+/linalool reaction have an m/z value of 137 (water-eliminated proton transfer product) and 81 (fragment ion) as well [11,12]. The H_3O^+/linalool reaction has a small reaction product at m/z 155 (protonated linalool), but since its contribution is at most 5% [12], rapid quantification of small amounts of this trace gas – as is for instance required in direct eddy covariance flux measurements of this compound above forest canopies – is expected to be highly inaccurate when it is based on the PTR-MS estimator ion of linalool at m/z 155.

In order to resolve this spectral interference, a reactant ion with differences in its reaction characteristics towards monoterpenes on one hand and linalool on the other needs to be found, be it differences in reaction rate constants and/or differences in the reaction products formed.

As already mentioned above, when using H_3O^+ as a source ion, protonated water clusters ($H_3O^+\cdot(H_2O)_n$, $n>1$) are readily formed when sampling ambient air and can complicate quantification due to differences in ion chemistry [13]. This is the case in SIFT-MS and APCI-MS, but also in PTR-MS at lower drift tube voltages.

Large differences in reaction rate constants of protonated water clusters with volatile organic compounds have previously been observed [14] and differences in product ions have been reported for the reactions of protonated water clusters with unsaturated C_5 and C_6 alcohols [15].

In addition, promising reports published in the literature show the possible applicability of protonated ethanol clusters $(C_2H_5OH)_mH^+$ as a selective reagent ion. Indeed, Aznar et al. [16] found clear differences in sensitivities between the monoterpene limonene and linalool as a function of the amount of ethanol added to an APCI source. Apart from this APCI-MS study, the efficiency of protonated ethanol clusters as CIMS reagent ions has also been demonstrated in a few other studies. Nowak et al. [17] reported the successful application of $(C_2H_5OH)_mH^+$ for the detection of dimethylsulfoxide, an oxidation product of dimethyl sulfide, and ammonia in ambient air and also suggested the use of ethanol clusters for the distinction between methyl vinyl ketone and methacrolein, two main oxidation products of isoprene. In both studies, the reagent $(C_2H_5OH)_nH^+$ cluster ions were declustered after passing the reaction zone, implying that the actual cluster ion distribution in the reaction region cannot be accurately known. Therefore, no accurate information concerning the characteristics of the occurring reactions could be derived. More recently, protonated ethanol clusters have been used by Boscaini et al. [18] for the detection of volatiles from the headspace of ethanolic solutions by PTR-MS. However, due to lack of data on the occurring ion/molecule reactions, no quantification of the measured compounds could be achieved. Dryahina et al. [19] very recently addressed the applicability of protonated ethanol clusters for the quantification of methylamine by SIFT-MS.

The need for a well-suited CIMS reagent ion which allows monoterpenes and linalool to be distinguished from one another, as well as the abovementioned observations reported in the literature, formed the foundation for the experimental study of the reactions of the monoterpene α-pinene and linalool with $H_3O^+\cdot(H_2O)_n$ ($n=1$–3), $(C_2H_5OH)_mH^+$ ($m=1$–3) and $(C_2H_5OH\cdot H_2O)H^+$ reagent ions in a flowing afterglow-selected ion flow tube instrument (FA-SIFT) [15]. Since α-pinene is known to be one of the major monoterpenes emitted on a global scale, it was chosen as a representative for this class of compounds in the present study. Rate constants and product ion distributions will be presented and the possible applicability for selective detection and accurate quantification by CIMS techniques will be discussed.

2. Experimental setup

2.1. Instrumentation: FA-SIFT

The FA-SIFT instrument that was used for the present ion/molecule reaction study has already been thoroughly described in a previous paper [15]. Consequently, only a short description addressing the most important features will be given here. The FA-SIFT instrument consists of four major parts: a flowing afterglow (FA) ion source, a reactant ion selection zone, a flow tube reactor zone and an ion detection section.

In the FA ion source, Ar atoms are ionized by electron impact ionization. The primary Ar^+ ions are converted to SIFT reactant ions by adding appropriate amounts of suitable neutral reactants to the afterglow. The reactant ions are subsequently sampled into the reactant ion selection zone, where they are separated according to their m/z ratio by a selection quadrupole mass filter. By means of a Venturi injector, the preselected reactant ions are then introduced into the SIFT reactor, in which they are convectively transported by a high ($100\,STP\,cm^3\,s^{-1}$) He carrier gas flow. The pressure in the SIFT reactor is maintained at 1.4 hPa. Two reactant gas inlets at different locations in the flow tube enable the measurement of reaction rate constants and product ion distributions. At the downstream end of the reactor, the source and product ions are sampled into the detection zone, where they are separated according to m/z ratio by a second quadrupole filter and detected by an electron multiplier.

2.2. Production of protonated ethanol clusters and their injection in the SIFT reactor

Protonated water and ethanol cluster ions are created by adding appropriate amounts of water and/or ethanol to the FA source. After pre-selection in the quadrupole mass filter, these clusters can undergo collision-induced dissociation in the vicinity of the injection orifice by collisions with backstreaming helium gas from the SIFT reactor when they are being injected in the reactor zone. The energy in the center of mass frame of these ions near the injector orifice (E_{CM}, in eV) is determined by the potential difference between the FA ion sampling plate and the SIFT injector plate (E_{LAB}) and the masses of the interacting particles.

The graphs of the absolute count rates and relative contributions of source/fragment ions versus E_{CM} of the corresponding source ions for the introduction of $H_3O^+\cdot(H_2O)_n$ ($n=1$–3) ions and the discussion thereof can be found in Ref. [15].

For $(C_2H_5OH)_mH^+$ ($m=1$–3) and $(C_2H_5OH\cdot H_2O)H^+$, the graphs are given in Fig. 1. The optimum E_{CM} value for the introduction of an ion presented here was chosen as a function of their applicability for the correct determination of the reaction rates and the product ion distributions. To this end, a sufficiently high reactant ion signal (>500 cps) and a minor contribution of impurities to the spectrum (<10%) were necessary. A value of E_{CM} meeting these requirements could easily be found for $C_2H_5OH_2^+$ and $(C_2H_5OH)_2H^+$ (Fig. 1a and c) at 1.0 and 0.55 eV, respectively. On the other hand, the easy ligand loss encountered when introducing $(C_2H_5OH\cdot H_2O)H^+$ and $(C_2H_5OH)_3H^+$ ions (Fig. 1b and d) demanded the use of a lower E_{CM}

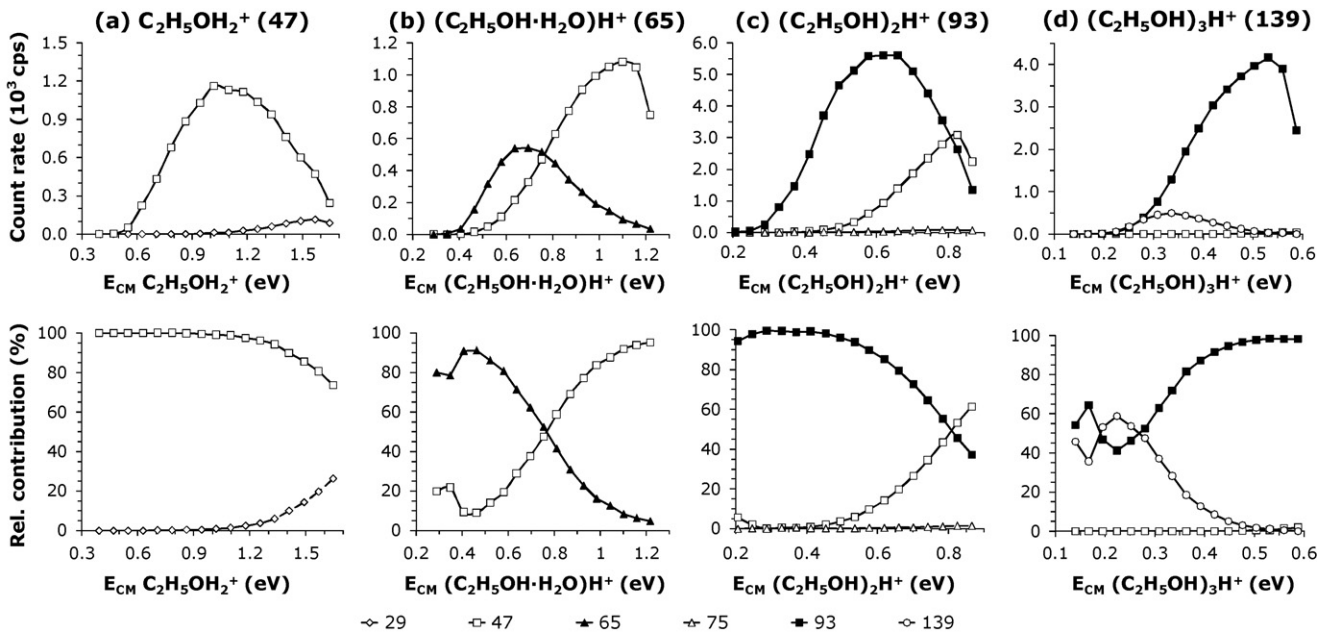

Fig. 1. Count rate (above) and relative contribution (below) of CID products encountered when injecting $C_2H_5OH_2^+$ (a), $(C_2H_5OH{\cdot}H_2O)H^+$ (b), $(C_2H_5OH)_2H^+$ (c) and $(C_2H_5OH)_3H^+$ (d) as a function of E_{CM} of the injected ion.

value (0.57 and 0.28 eV, respectively) to obtain both a workable count rate and purity.

2.3. Measuring methods

Reaction rate constants and product ion distributions (PID) have been determined at room temperature (298 K) according to the methods described previously [15].

Reproducible reaction rate constants have been obtained by introducing volumetric mixtures of the reactant neutrals in He, prepared in volume-calibrated glass bottles, into the flow tube through a heated (40 °C) needle valve. The reactant gas flow was determined by the pressure decay in the glass bottles as a function of time and for each reaction, at least three different mixing ratios were used. Rate constants have been obtained from the logarithmic decay of the reactant ion signal as a function of the compound concentration in the flow tube. The reaction time, needed to calculate the rate constants, has been determined experimentally and was found to be 2.8 ms at typical conditions of flow rate and pressure in the SIFT reactor.

Product ion distributions (PID) were determined by operating the mass spectrometer in the multi-ion-mode (MIM) and by introducing the compounds at the inlet close to the downstream mass spectrometer inlet orifice to minimize distortion by diffusion enhancement effects and possible secondary reactions.

As usual, corrections for background, isotopic abundances and mass discrimination have been applied. The PIDs of the reactions have been corrected for the contributions of product ions originating from declustered reactant ions (generally loss of one ligand) by taking into account the accurate PIDs of the reactions with those declustered ions, the ratio of these declustered ions to the sum of all ions in the SIFT reactor and the differences in rate constants between the declustered ions and the clusters.

2.4. Chemicals used

Linalool (97%, Aldrich) and α-pinene (99%, Aldrich) were obtained commercially as indicated. Ar and He buffer gases were obtained from Air Products and have a stated purity of 99.9997%.

3. Results

In the tables presented below (Tables 1–4), experimentally obtained reaction rate constants (k_{EXP}) are compared to calculated collision rate constants (k_{COL}) obtained with the parameterized theory of Su and Chesnavich [20,21]. In this theory, collision rate

Table 1
Product ion distributions, experimental rate constants (k_{EXP}) and calculated collision rate constants (k_{COL}) for the reactions of α-pinene ($C_{10}H_{16}$) with the protonated water clusters $H_3O^+{\cdot}(H_2O)_n$ (n = 1–3). Values for the H_3O^+/α-pinene reaction taken from Ref. [9]. N/A: no product ions could be identified due to the very low experimental reaction rate.

Reactant ion (m/z)	Product ion distribution		Reaction rate constants (10^{-9} molecule^{-1} cm^3 s^{-1})
	Product ions (m/z)	(%)	k_{EXP} [k_{COL}]
H_3O^+ (19)	$C_6H_9^+$ (81)	30	2.3 [2.4]
	$C_{10}H_{17}^+$ (137)	67	
	Other	3	
$H_3O^+{\cdot}H_2O$ (37)	$C_{10}H_{17}^+$ (137)	99	1.8 [1.8]
	Other	1	
$H_3O^+{\cdot}(H_2O)_2$ (55)	$C_{10}H_{17}^+$ (137)	86	1.6 [1.6]
	$(C_{10}H_{16}{\cdot}H_2O)H^+$ (155)	13	
	Other	1	
$H_3O^+{\cdot}(H_2O)_3$ (73)	N/A	N/A	0.074 [1.4]

Table 2
Product ion distributions, experimental rate constants (k_{EXP}) and calculated collision rate constants (k_{COL}) for the reactions of linalool ($C_{10}H_{18}O$) with the protonated water clusters $H_3O^+\cdot(H_2O)_n$ (n = 1–3). Values for the H_3O^+/linalool reaction taken from Ref. [12]. (*) Large uncertainty on values (see text).

Reactant ion (m/z)	Product ion distribution		Reaction rates constants (10^{-9} molecule^{-1} cm^3 s^{-1})
	Product ions (m/z)	(%)	k_{EXP} [k_{COL}]
H_3O^+ (19)	$C_3H_7O^+$ (59)	2	3.0 [3.2]
	$C_5H_9^+$ (69)	2	
	$C_6H_9^+$ (81)	30	
	$C_7H_{11}^+$ (95)	2	
	$C_{10}H_{17}^+$ (137)	56	
	$C_{10}H_{19}O^+$ (155)	4	
	Other	4	
$H_3O^+\cdot H_2O$ (37)	$C_6H_9^+$ (81)	2	2.3 [2.4]
	$C_{10}H_{17}^+$ (137)	91	
	$C_{10}H_{19}O^+$ (155)	7	
$H_3O^+\cdot(H_2O)_2$ (55)	$C_{10}H_{17}^+$ (137)	31	1.9 [2.1]
	$C_{10}H_{19}O^+$ (155)	3	
	$(C_{10}H_{18}O\cdot H_2O)H^+$ (173)	66	
$H_3O^+\cdot(H_2O)_3$ (73)	$C_{10}H_{17}^+$ (137)	30(*)	1.6 [1.6]
	$(C_{10}H_{18}O\cdot H_2O)H^+$ (173)	35(*)	
	$(C_{10}H_{18}O\cdot(H_2O)_2)H^+$ (191)	25(*)	
	Other	10(*)	

Table 3
Product ion distributions, experimental rate constants (k_{EXP}) and calculated collision rate constants (k_{COL}) for the reactions of α-pinene ($C_{10}H_{16}$) with the protonated ethanol clusters $(C_2H_5OH)_mH^+$ (m = 1–3) and $(C_2H_5OH\cdot H_2O)H^+$. N/A: no product ions could be identified due to the very low experimental reaction rate.

Reactant ion (m/z)	Product ion distribution		Reaction rates constants (10^{-9} molecule^{-1} cm^3 s^{-1})
	Product ions (m/z)	(%)	k_{EXP} [k_{COL}]
$C_2H_5OH_2^+$ (47)	$C_{10}H_{17}^+$ (137)	99	1.5 [1.7]
	Other	1	
$(C_2H_5OH\cdot H_2O)H^+$ (65)	$C_{10}H_{17}^+$ (137)	98	1.4 [1.5]
	Other	2	
$(C_2H_5OH)_2H^+$ (93)	$C_{10}H_{17}^+$ (137)	58	0.72 [1.3]
	$(C_{10}H_{16}\cdot C_2H_5OH)H^+$ (183)	42	
$(C_2H_5OH)_3H^+$ (139)	N/A	N/A	0.055 [1.2]

constants are calculated using the polarizability and electric dipole moment of the compound. As no experimental values are available for α-pinene and linalool, values from Schoon et al. [9] and Amelynck et al. [12] obtained from quantum chemical calculations, were used. Also, results concerning the PIDs of the reactions of H_3O^+ with α-pinene and linalool were taken from these articles. The estimated uncertainty on the experimentally determined rate constants is 25%. The estimated uncertainty of the published branching ratios is at most 12% and decreases to 5% for branching ratios above 25%, except for the reactions with $H_3O^+\cdot(H_2O)_3$ for which, due to the mathematical correction and the low $H_3O^+\cdot(H_2O)_3$ purity (15%), the uncertainty was 25% for the most abundant channels and increases to 50% for the less abundant channels. Due to these uncertainties, only product ions with a yield equal to 2% or larger are considered for all reactions except for the $H_3O^+\cdot(H_2O)_3$ reactions, for which only product ions with a yield larger than 5% are taken into account.

Table 4
Product ion distributions, experimental rate constants (k_{EXP}) and calculated collision rate constants (k_{COL}) for the reactions of linalool ($C_{10}H_{18}O$) with the protonated ethanol clusters $(C_2H_5OH)_mH^+$ (m = 1–3) and $(C_2H_5OH\cdot H_2O)H^+$.

Reactant ion (m/z)	Product ion distribution		Reaction rates constants (10^{-9} molecule^{-1} cm^3 s^{-1})
	Product ions (m/z)	(%)	k_{EXP} [k_{COL}]
$C_2H_5OH_2^+$ (47)	$C_6H_9^+$ (81)	10	2.1 [2.2]
	$C_{10}H_{17}^+$ (137)	87	
	Other	3	
$(C_2H_5OH\cdot H_2O)H^+$ (65)	$C_{10}H_{17}^+$ (137)	55	1.9 [1.9]
	$C_{10}H_{19}O^+$ (155)	2	
	$(C_{10}H_{18}O\cdot H_2O)H^+$ (173)	3	
	$(C_{10}H_{16}\cdot C_2H_5OH)H^+$ (183)	22	
	$(C_{10}H_{18}O\cdot C_2H_5OH)H^+$ (201)	16	
$(C_2H_5OH)_2H^+$ (93)	$C_{10}H_{17}^+$ (137)	14	1.7 [1.7]
	$(C_{10}H_{16}\cdot C_2H_5OH)H^+$ (183)	9	
	$(C_{10}H_{18}O\cdot C_2H_5OH)H^+$ (201)	77	
$(C_2H_5OH)_3H^+$ (139)	$C_{10}H_{17}^+$ (137)	10	1.6 [1.5]
	$(C_{10}H_{18}O\cdot C_2H_5OH)H^+$ (201)	87	
	Other	3	

3.1. $H_3O^+\cdot(H_2O)_n$ (n = 1–3) reactions

In Tables 1 and 2, the product ion distributions and the rate constants for the reactions of $H_3O^+\cdot(H_2O)_n$ (n = 1–3) clusters with α-pinene and linalool, respectively, are given.

Proton transfer from $H_3O^+\cdot H_2O$ can only proceed if the proton affinity of the compound is larger than 810 kJ mol^{-1}. This value was obtained using the proton affinity of water (691 kJ mol^{-1} [22]), the H_3O^+–H_2O bond energy (134 kJ mol^{-1} [23]) and the H_2O–H_2O bond energy (15 kJ mol^{-1} [24]). As less excess energy is available for fragmentation, $H_3O^+\cdot H_2O$ is a softer ionization reagent compared to the bare H_3O^+ ion.

The $H_3O^+\cdot H_2O$/α-pinene reaction yields almost exclusively protonated α-pinene (reaction (1)). The protonated linalool yield for the $H_3O^+\cdot H_2O$/linalool reaction is low (reaction (2c)) and proton transfer followed by water elimination (reaction (2b)) is the major pathway:

$$\alpha\text{-Pinene} + H_3O^+\cdot H_2O \rightarrow C_{10}H_{17}^+ + 2H_2O \quad (99\%) \qquad (1)$$

$$\text{Linalool} + H_3O^+\cdot H_2O \rightarrow C_6H_9^+ + C_4H_8 + 3H_2O \quad (2\%) \qquad (2a)$$

$$\text{Linalool} + H_3O^+\cdot H_2O \rightarrow C_{10}H_{17}^+ + 3H_2O \quad (91\%) \qquad (2b)$$

$$\text{Linalool} + H_3O^+\cdot H_2O \rightarrow C_{10}H_{19}O^+ + 2H_2O \quad (7\%) \qquad (2c)$$

The $H_3O^+\cdot(H_2O)_2$/α-pinene reactions (Table 1) mainly result in the protonated compound (reaction (3a)) and the water-eliminated ligand switching product (reaction (3b)). For the $H_3O^+\cdot(H_2O)_2$/linalool reaction, major ions are the ligand switching product followed by elimination of a water ligand (reaction (4c)) and the proton transfer product followed by water elimination (reaction (4a)). Protonated linalool was again only a minor product (reaction (4b)):

$$\alpha\text{-Pinene} + H_3O^+\cdot(H_2O)_2 \rightarrow C_{10}H_{17}^+ + 3H_2O \quad (86\%) \qquad (3a)$$

$$\alpha\text{-Pinene} + H_3O^+\cdot(H_2O)_2 \rightarrow (C_{10}H_{16}\cdot H_2O)H^+ + 2H_2O \quad (13\%) \qquad (3b)$$

$$\text{Linalool} + H_3O^+\cdot(H_2O)_2 \rightarrow C_{10}H_{17}^+ + 4H_2O \quad (31\%) \qquad (4a)$$

$$\text{Linalool} + H_3O^+\cdot(H_2O)_2 \rightarrow C_{10}H_{19}O^+ + 3H_2O \quad (3\%) \qquad (4b)$$

$$\text{Linalool} + H_3O^+\cdot(H_2O)_2 \rightarrow (C_{10}H_{18}O\cdot H_2O)H^+ + 2H_2O \quad (66\%) \qquad (4c)$$

A large difference was found between the rate constants for reaction of $H_3O^+\cdot(H_2O)_3$ with the respective compounds. Linalool was found to react with a rate constant close to the collision limit, but the reaction rate of α-pinene was about 20 times slower than the collision limit. This also implied that the product ions could not be determined for the latter reaction. The $H_3O^+\cdot(H_2O)_3$/linalool reactions result in major ions for the ligand switching product followed by elimination of one (reaction (5c)) or two (reaction (5b)) water ligands and the proton transfer product followed by water elimination (reaction (5a)):

$$\text{Linalool} + H_3O^+\cdot(H_2O)_3 \rightarrow C_{10}H_{17}^+ + 5H_2O \quad (30\%) \qquad (5a)$$

$$\text{Linalool} + H_3O^+\cdot(H_2O)_3 \rightarrow (C_{10}H_{18}O\cdot H_2O)H^+ + 3H_2O \quad (35\%) \qquad (5b)$$

$$\text{Linalool} + H_3O^+\cdot(H_2O)_3 \rightarrow (C_{10}H_{18}O\cdot(H_2O)_2)H^+ + 2H_2O \quad (25\%) \qquad (5c)$$

3.2. $(C_2H_5OH)_mH^+$ (m = 1–3) and $(C_2H_5OH\cdot H_2O)H^+$ reactions

In Tables 3 and 4, the product ion distributions and the rate constants for the reactions of $(C_2H_5OH)_mH^+$ (m = 1–3) and $(C_2H_5OH\cdot H_2O)H^+$ reactions with α-pinene and linalool are presented, respectively.

The proton affinity of ethanol ($PA_{C_2H_5OH}$ = 776.4 kJ mol^{-1} [22]) is higher than the proton affinity of water (PA_{H_2O} = 691 kJ mol^{-1} [22]) and lower than the energy needed for proton transfer from $H_3O^+\cdot H_2O$ (810 kJ mol^{-1}). The reaction of protonated ethanol with α-pinene and linalool is therefore expected to result in less fragmentation than the H_3O^+ reactions, but more than the $H_3O^+\cdot H_2O$ reactions, which is confirmed in the results.

The reactions of $C_2H_5OH_2^+$ with α-pinene and linalool both occur at the collision rate.

The $C_2H_5OH_2^+$/α-pinene reaction almost exclusively results in the proton transfer product (reaction (6)) and the $C_2H_5OH_2^+$/linalool reaction has major ions for the proton transfer product followed by water elimination (reaction (7b)) and the fragment at m/z 81 (reaction (7a)):

$$\alpha\text{-Pinene} + C_2H_5OH_2^+ \rightarrow C_{10}H_{17}^+ + C_2H_5OH \quad (99\%) \qquad (6)$$

$$\text{Linalool} + C_2H_5OH_2^+ \rightarrow C_6H_9^+ + C_4H_8 + H_2O + C_2H_5OH \quad (10\%) \qquad (7a)$$

$$\text{Linalool} + C_2H_5OH_2^+ \rightarrow C_{10}H_{17}^+ + H_2O + C_2H_5OH \quad (87\%) \qquad (7b)$$

The reactions of $(C_2H_5OH\cdot H_2O)H^+$ with both compounds were found to proceed at the collision rate.

The reaction of $(C_2H_5OH\cdot H_2O)H^+$ with α-pinene mainly results in the protonated product (98%, reaction (8)).

For the $(C_2H_5OH\cdot H_2O)H^+$/linalool reactions, major ions were the proton transfer product followed by water elimination (reaction (9a)), the water ligand switching product followed by elimination of one water molecule (reaction (9d)) and the water ligand switching reaction (reaction (9e)). Also, minor channels were observed for the proton transfer product (reaction (9b)) and the ethanol ligand switching channel (reaction (9c)):

$$\alpha\text{-Pinene} + (C_2H_5OH\cdot H_2O)H^+ \rightarrow C_{10}H_{17}^+ + H_2O + C_2H_5OH \quad (98\%) \qquad (8)$$

$$\text{Linalool} + (C_2H_5OH\cdot H_2O)H^+ \rightarrow C_{10}H_{17}^+ + 2H_2O + C_2H_5OH \quad (55\%) \qquad (9a)$$

$$\text{Linalool} + (C_2H_5OH\cdot H_2O)H^+ \rightarrow C_{10}H_{19}O^+ + H_2O + C_2H_5OH \quad (2\%) \qquad (9b)$$

$$\text{Linalool} + (C_2H_5OH\cdot H_2O)H^+ \rightarrow (C_{10}H_{18}O\cdot H_2O)H^+ + C_2H_5OH \quad (3\%) \qquad (9c)$$

$$\text{Linalool} + (C_2H_5OH\cdot H_2O)H^+ \rightarrow (C_{10}H_{16}\cdot C_2H_5OH)H^+ + 2H_2O \quad (22\%) \qquad (9d)$$

$$\text{Linalool} + (C_2H_5OH\cdot H_2O)H^+ \rightarrow (C_{10}H_{18}O\cdot C_2H_5OH)H^+ + H_2O \quad (16\%) \qquad (9e)$$

The reaction of the protonated ethanol dimer with linalool occurs at the collision rate. The reaction with α-pinene, however, proceeds at a rate about half the collision rate.

The reaction of α-pinene with the protonated ethanol dimer proceeds by proton transfer (reaction (10a)) and ligand switching (reaction (10b)). The linalool/$(C_2H_5OH)_2H^+$ reaction proceeds by proton transfer followed by water elimination (reaction (11a)), ligand switching followed by water elimination (reaction (11b)) and ligand switching (reaction (11c)):

$$\alpha\text{-Pinene} + (C_2H_5OH)_2H^+ \rightarrow C_{10}H_{17}^+ + 2\,C_2H_5OH \quad (58\%) \qquad (10a)$$

$$\alpha\text{-Pinene} + (C_2H_5OH)_2H^+ \rightarrow (C_{10}H_{16}{\cdot}C_2H_5OH)H^+ + C_2H_5OH \quad (42\%) \tag{10b}$$

$$\text{Linalool} + (C_2H_5OH)_2H^+ \rightarrow C_{10}H_{17}{}^+ + H_2O + 2C_2H_5OH \quad (14\%) \tag{11a}$$

$$\text{Linalool} + (C_2H_5OH)_2H^+ \rightarrow (C_{10}H_{16}{\cdot}C_2H_5OH)H^+ + H_2O + C_2H_5OH \quad (9\%) \tag{11b}$$

$$\text{Linalool} + (C_2H_5OH)_2H^+ \rightarrow (C_{10}H_{18}O{\cdot}C_2H_5OH)H^+ + C_2H_5OH \quad (77\%) \tag{11c}$$

The reaction of the protonated ethanol trimer with linalool also occurs at the collision rate. The reaction with α-pinene, however, proceeds at a rate which is only 5% of the collision rate.

The linalool/$(C_2H_5OH)_3H^+$ reaction mechanisms are proton transfer followed by water elimination (reaction (12a)) and ligand switching (reaction (12b)) with elimination of ethanol:

$$\text{Linalool} + (C_2H_5OH)_3H^+ \rightarrow C_{10}H_{17}{}^+ + H_2O + 3C_2H_5OH \quad (10\%) \tag{12a}$$

$$\text{Linalool} + (C_2H_5OH)_3H^+ \rightarrow (C_{10}H_{18}O\,C_2H_5OH)H^+ + 2C_2H_5OH \quad (87\%) \tag{12b}$$

4. Discussion

In what follows, the experimental results obtained in the present study will be discussed in view of their possible applicability for quantification of α-pinene and linalool and α-pinene/linalool distinction using CIMS techniques. The ion chemistry data will also be used to clarify some of the observations reported concerning the differences in detection sensitivity of limonene and linalool as a function of the make-up gas ethanol content in an APCI-MS instrument by Aznar et al. [16]. Although our FA-SIFT study focused onto α-pinene instead of limonene, all H_3O^+/monoterpene reactions investigated thus far occur at the collision rate and result in the same product ions (*m*/*z* 137 and *m*/*z* 81), albeit with different branching ratios [8–11]. Therefore, it is relatively safe to assume that the product ions resulting from the reactions of protonated clusters with monoterpenes other than α-pinene will be similar.

4.1. $H_3O^+{\cdot}(H_2O)_n$ (n = 0–3) reactions

The reactions of α-pinene with both $H_3O^+{\cdot}H_2O$ and $H_3O^+{\cdot}(H_2O)_2$ have a higher branching ratio for the reaction channel resulting in protonated α-pinene (*m*/*z* 137) than the one with bare H_3O^+, but their rate constants are somewhat lower. Consequently, in case the ion signal at *m*/*z* 137 is only due to monoterpenes, only a small improvement of the monoterpene detection sensitivity based on this ion signal can be expected when using instrumental conditions at which $H_3O^+{\cdot}H_2O$ and $H_3O^+{\cdot}(H_2O)_2$ dominate the reactant ion distribution. Loss of the product ion species at *m*/*z* 137 ($C_{10}H_{17}{}^+$) by hydration in the CIMS reactor, which could offset this improvement, is not expected to be important since hydrocarbon ions have no propensity to hydrate [14].

When α-pinene and linalool are simultaneously present in the sample to be analysed, quantification of one or both of these compounds using $H_3O^+{\cdot}(H_2O)_n$ ion chemistry becomes difficult, if not impossible. Indeed, the H_3O^+/linalool reaction mainly results in identical product ions as the H_3O^+/α-pinene reaction. The H_3O^+/linalool reaction also results in protonated linalool, but the branching ratio for this channel is very small and may lead to a very inaccurate quantification of linalool when present at very low concentrations. Increasing the contribution of $H_3O^+{\cdot}H_2O$ reactant ions in a CIMS instrument (by adding water vapour or, in particular for PTR-MS instruments by decreasing the E/N value in the drift tube reactor) does not help to distinguish the two compounds since both the $H_3O^+{\cdot}H_2O$/α-pinene and the $H_3O^+{\cdot}H_2O$/linalool reactions mainly result in a product ion at *m*/*z* 137 (99% for α-pinene and 91% for linalool).

Since large differences between the reaction rate constants of $H_3O^+{\cdot}(H_2O)_3$ with α-pinene and linalool have been observed, the use of instrumental conditions at which this ion species dominates the proton hydrate reactant ion distribution could possibly lead to the selective detection of linalool.

4.2. $(C_2H_5OH)_mH^+$ (m = 1–3) and $(C_2H_5OH{\cdot}H_2O)H^+$ reactions

The reactions of α-pinene with both $C_2H_5OH_2{}^+$ and $(C_2H_5OH{\cdot}H_2O)H^+$ have a higher branching ratio for the channel resulting in protonated α-pinene (*m*/*z* 137) than the H_3O^+/α-pinene reaction. Because of the difference in rate constants, however, this does not necessarily imply a higher detection sensitivity for α-pinene based on the ion signal at *m*/*z* 137 when using the former two ions as CIMS reactant ions. Furthermore, the reactions of both $C_2H_5OH_2{}^+$ and $(C_2H_5OH{\cdot}H_2O)H^+$ with linalool primarily result in the proton transfer product followed by water elimination, at *m*/*z* 137, which again complicates monoterpene quantification in the presence of linalool.

CIMS conditions at which $(C_2H_5OH)_3H^+$ dominates the $(C_2H_5OH)_mH^+$ reactant ion distribution might be useful for quantification of linalool due to the high contribution of the ligand switching product followed by ethanol elimination (*m*/*z* 201, 87%) and the very low reaction rate for the $(C_2H_5OH)_3H^+$/α-pinene reaction.

4.3. Interpretation of APCI results for detection of limonene and linalool

The results concerning ion/molecule reactions obtained in the present work can help to explain the large differences in detection sensitivity between limonene and linalool that were observed by Aznar et al. [16] when using $(C_2H_5OH)_nH^+$ reactant ion clusters in their APCI-MS instrument [25].

Due to the complexity of the competing reactions that occur in the system and the fragmentation and declustering caused by the cone voltage applied in the APCI-MS, a complete and decisive explanation of the observed limonene and linalool product ion signal variations as a function of the amount of ethanol added to the source is impossible. However, combination of their results with the ones presented here may provide additional information for the discussion of some clearly observed trends.

Our results on α-pinene can for instance provide an explanation for the experimentally observed intensity decrease of the limonene product ion signal at *m*/*z* 137 as a function of the ethanol concentration in the APCI-MS instrument. Indeed, an increase in ethanol concentration results in a shift of the $(C_2H_5OH)_mH^+$ reactant cluster ion distribution towards higher order clusters and the rate constants of monoterpenes (exemplified by α-pinene in the present study) were found to decrease firmly as a function of cluster size. Consequently less product ions at *m*/*z* 137 will be formed when increasing the ethanol concentration in the APCI-MS system at constant limonene concentrations.

In contrast to α-pinene, the reactions of higher order $(C_2H_5OH)_mH^+$ clusters with linalool continue to proceed at the collision limit (at least up to *m* = 3). As a result, the linalool product ions are not expected to firmly decrease as a function of

the concentration of the ethanol make-up gas. Aznar et al. [16] reported an intensity increase of the linalool product ion at m/z 137 and a gradual decrease of the one at m/z 81 as a function of the ethanol concentrations. This suggests that higher order $(C_2H_5OH)_mH^+$/linalool product ions will mainly decluster and/or fragment to ions at m/z 137 at the energetic conditions of the APCI-MS instrument.

The drastic intensity decrease of the ion signal at m/z 137 for limonene, the increase at m/z 137 for linalool and the gradual decrease at m/z 81 for linalool observed as a function of the ethanol content by Aznar et al. [16] all suggest the presence of even larger order ethanol clusters ($m > 3$) in the APCI-MS ion source with even lower reaction rates for limonene.

5. Conclusions

The reactions of $H_3O^+\cdot(H_2O)_n$ ($n = 0–3$) and $(C_2H_5OH)_mH^+$ ($m = 1–3$) with α-pinene and linalool have been studied in a FA-SIFT instrument at 1.4 hPa and 298 K. All reactions with linalool were found to occur at the collision limit. The $(C_2H_5OH)_2H^+$/α-pinene proceeds at half the collision rate and both the $(C_2H_5OH)_3H^+$/α-pinene and $H_3O^+\cdot(H_2O)_3$/α-pinene reaction have a very low rate constant. All other reactions involving α-pinene proceed at the collision rate.

The results also reveal that a high contribution of $H_3O^+\cdot H_2O$ ions in the proton hydrate reactant ion distribution leads to an increase in detection sensitivity for both α-pinene and linalool based on the ion signal at m/z 137, compared to using bare H_3O^+ reactant ions. This is in agreement with the observations of Tani et al. [26] who observed an increase in detection sensitivity for α-pinene (based on the ion signal at m/z 137) due to changes in the proton hydrate distribution induced by lowering the E/N value in the PTR-MS reactor. Application of protonated ethanol as CIMS reactant ion will also result in an small improvement of the detection sensitivity for linalool based on the ion signal at m/z 137.

The rate constants and product ion distributions obtained in this work indicate that differentiation of monoterpenes and linalool with CIMS instrumentation using protonated water clusters or protonated ethanol clusters as reactant ions is not straightforward. However, it should be possible to accurately determine linalool emissions in conditions at which the protonated ethanol trimer dominates the reactant ion spectrum. Such conditions can be obtained in existing APCI-MS [16] and SIFT-MS [19] instrumentation. An instrument which is capable to switch between conditions at which on the one hand $(C_2H_5OH)_3H^+$ or on the other hand $H_3O^+\cdot H_2O$ or $C_2H_5OH_2^+$ ions dominate the reactant ion spectrum should therefore allow to quantify both compounds with a reasonable accuracy.

Further optimization of the proposed method for linalool/α-pinene differentiation will require additional studies on the hydration of the ethanol cluster source ions and the product ions in humid samples.

Acknowledgements

This research was supported by the Institute for the Promotion of Innovation through Science and Technology in Flanders (IWT-Vlaanderen) and by the Belgian Federal Science Policy Office (Project # MO/35/022 & # MO/35/026).

References

[1] A. Guenther, C.N. Hewitt, D. Erickson, R. Fall, C. Geron, T. Graedel, P. Harley, L. Klinger, M. Lerdau, W.A. Mckay, T. Pierce, B. Scholes, R. Steinbrecher, R. Tallamraju, J. Taylor, P. Zimmerman, J. Geophys. Res. 100 (1995) 8873–8892.
[2] R.J. Griffin, D.R. Cocker III, R.C. Flagan, J.H. Seinfeld, J. Geophys. Res. 104 (1999) 3555–3567.
[3] M. Kanakidou, J.H. Seinfeld, S.N. Pandis, I. Barnes, F.J. Dentener, M.C. Facchini, R. Van Dingenen, B. Ervens, A. Nenes, C.J. Nielsen, E. Swietlicki, J.P. Putaud, Y. Balkanski, S. Fuzzi, J. Horth, G.K. Moortgat, R. Winterhalter, C.E.L. Myhre, K. Tsigaridis, E. Vignati, E.G. Stephanou, J. Wilson, Atmos. Chem. Phys. 5 (2005) 1053–1123.
[4] N.L. Ng, J.H. Kroll, M.D. Keywood, R. Bahreini, V. Varutbangkul, R.C. Flagan, J.H. Seinfeld, A. Lee, A.H. Goldstein, Environ. Sci. Technol. 40 (2006) 2283–2297.
[5] W. Lindinger, A. Jordan, Chem. Soc. Rev. 27 (1998) 347–375.
[6] D. Smith, P. Španel, Mass Spectrom. Rev. 24 (2005) 661–700.
[7] A.J. Taylor, R.S.T. Linforth, B.A. Harvey, A. Blake, Food Chem. 71 (2000) 327–338.
[8] T. Wang, P. Španel, D. Smith, Int. J. Mass Spectrom. 228 (2003) 117–126.
[9] N. Schoon, C. Amelynck, L. Vereecken, E. Arijs, Int. J. Mass Spectrom. 229 (2003) 231–240.
[10] A. Tani, S. Hayward, C.N. Hewitt, Int. J. Mass Spectrom. 223–224 (2003) 561–578.
[11] S.D. Maleknia, T.L. Bell, M.A. Adams, Int. J. Mass Spectrom. 262 (2007) 203–210.
[12] C. Amelynck, N. Schoon, T. Kuppens, P. Bultinck, E. Arijs, Int. J. Mass Spectrom. 247 (2005) 1–9.
[13] P. Španel, D. Smith, Rapid Commun. Mass Spectrom. 14 (2000) 1898–1906.
[14] P. Španel, D. Smith, J. Phys. Chem. 99 (1995) 15551–15556.
[15] F. Dhooghe, C. Amelynck, J. Rimetz-Planchon, N. Schoon, F. Vanhaecke, Int. J. Mass Spectrom. 285 (2009) 31–41.
[16] M. Aznar, M. Tsachaki, R.S.T. Linforth, V. Ferreira, A.J. Taylor, Int. J. Mass Spectrom. 239 (2004) 17–25.
[17] J.B. Nowak, L.G. Huey, F.L. Eisele, D.J. Tanner, E. Kosciuch, D.D. Davis, R. Mauldin III, C. Cantrell, J. Geophys. Res. 107 (2002) 4363.
[18] E. Boscaini, T. Mikoviny, A. Wisthaler, E. Hartungen, T.D. Märk, Int. J. Mass Spectrom. 239 (2004) 215–219.
[19] K. Dryahina, F. Pehal, D. Smith, P. Španel, Int. J. Mass Spectrom. 286 (2009) 1–6.
[20] T. Su, W.J. Chesnavich, J. Chem. Phys. 76 (1982) 5183–5185.
[21] T. Su, J. Chem. Phys. 88 (1988) 4102–4103.
[22] E.P.L. Hunter, S.G. Lias, J. Phys. Chem. Ref. Data 27 (1998) 413–656.
[23] A.J. Cunningham, J.D. Payzant, P. Kebarle, J. Am. Chem. Soc. 94 (1972) 7627–7632.
[24] L.A. Curtiss, D.J. Frurip, M. Blander, J. Chem. Phys. 71 (1979) 2703–2711.
[25] R.S.T. Linforth, A.J. Taylor, Apparatus and Methods for the Analysis of Trace Constituents in Gases, US Patent 5,869,344 (n.d.).
[26] A. Tani, S. Hayward, A. Hansel, C.N. Hewitt, Int. J. Mass Spectrom. 239 (2004) 161–169.